Available online at www.sciencedirect.com

SciVerse ScienceDirect

Ceramics International 38 (2012) 4935–4942

CERAMICS INTERNATIONAL

www.elsevier.com/locate/ceramint

Study on the new bone cement based on calcium sulfate and Mg, CO_3 doped hydroxyapatite

Aneta Zima *, Zofia Paszkiewicz, Dominika Siek, Joanna Czechowska, Anna Ślósarczyk

Faculty of Materials Science and Ceramics, AGH – University of Science and Technology, Cracow, Poland

Received 17 February 2012; accepted 27 February 2012
Available online 5 March 2012

Abstract

In order to improve some features of bone substitutes the new self-setting composite-type implant material based on Mg^{2+}/CO_3^{2-} co-substituted hydroxyapatite (Mg-CHA) and calcium sulfate hemihydrate (CSH) was developed. Synthetic hydroxyapatites doped with small amounts of additives found in natural bone (*e.g.* Mg^{2+} and CO_3^{2-}) are regarded as promising components of calcium phosphate bone cements (CPCs). The CPCs, now available on the market, due to low resorption rate are too stable to permit material degradation and are slowly replaced by the newly formed bone. To improve cement resorption we used calcium sulfate which is a well-known biodegradable and biocompatible bone defect filler. Combining properties of Mg-CHA and CSH allowed developing a new, promising, easy shapeable implant material with high potential for bone regeneration.

Keywords: B. Composites; Bone cement; Doped hydroxyapatite

1. Introduction

Self-setting calcium phosphate cements (CPCs) have been applied in bone repair for about 30 years. Due to excellent biocompatibility, bioactive properties as well as simplicity of preparation and use, they are popular in orthopedy, maxillofacial surgery and dentistry. A great number of CPCs with different powder and liquid phase compositions are commercially available but still many of them are at the experimental stages [1–6]. Depending on the final product obtained after setting, CPCs can be classified as: apatitic cements (HA – hydroxyapatite, CDHA – calcium deficient hydroxyapatite), brushite cements (DCPD – dicalcium phosphate dihydrate) and carbonated-apatitic cements (CHA – carbonated hydroxyapatite) [7,8]. The final setting product of cements is essential because it determines the solubility and resorbability of the biomaterial *in vivo*. The implanted calcium phosphate cements may be resorbed by two possible mechanisms: an active resorption – due to cellular activity of macrophages, osteoclasts, osteoblasts and other cells or a passive resorption – due to dissolution or hydrolysis (brushite cements) under physiological conditions [9–12]. Biological resorption of bone substitutes is mainly related to the solubility of individual phases. It is well known that brushite cements are faster degraded due to better solubility of DCPD in comparison with CDHA which is more stable in human environment [13–15]. *In vitro* and *in vivo* tests showed that these cements are well tolerated by bone tissue [16–19]. However, short setting times, low mechanical strength compared to apatite cements and poor injectability limit wider clinical applications of brushite cements.

There are several areas in the knowledge on bone cements that require more research. One of the main challenges for researches is to increase the resorption rate of apatitic cements and reach higher rate of new bone formation. Properties of cements can be improved by manipulating their chemical composition, changing particle size of initial powders, using various kinds of liquid phases with different liquid-to-powder ratio as well as by introducing various additives. The current commercial CPCs remain dense after implantation because of the absence of macroporosity which is needed for cell colonization and bone ingrowth. The problem with porosity (micro and macro) in this group of implant materials can be solved by incorporation of various soluble components, such as

* Corresponding author.
E-mail address: azima@agh.edu.pl (A. Zima).

0272-8842/$36.00
doi:10.1016/j.ceramint.2012.02.086

sugar, mannitol or resorbable fibers, into the cements [20–23]. However, after cement implantation and dissolving the soluble particles, pores created in the cement matrix are not always interconnected. Experimental results suggest that a number of parameters of calcium phosphate cements, *e.g.* carbonate content, ionic substitution and crystallinity, may affect the dissolution characteristics of these materials. This gives an opportunity to form cements varying in resorption rate, *i.e.* suitable for different medical applications [9].

Previous reports suggest that ion substitution in hydroxyapatite structure is one of the key parameters affecting physicochemical and biological properties (bioactivity, biocompatibility and biomaterial/tissue interactions) of HA ceramics [24,25]. Among different ions used as modifiers, Mg^{2+} and CO_3^{2-} seem to be very promising. Magnesium and carbonate groups are minor but important components of bone, enamel and dentine. Mg plays an essential role in the biological environment due to its significant impact on the mineralization process and also influence on HA crystal formation and growth [26]. Synthetic Mg-substituted CaPs are expected to produce enhanced biological and chemical responses in the body. When applied in bone cements, MgHA influences their properties. According to Lilley [27], the presence of magnesium has a strong effect on the cement composition and strength; it leads to an increase in brushite content and decrease in the compressive strength of hardened materials. Results of these studies suggest that Mg can be used to adjust the composition and rate of cement hydration. Magnesium has been reported to have a stabilizing role in non-crystalline CaPs. According to LeGeros incorporation of both, carbonate (CO_3) and Mg ions promotes formation and stabilization of ACP (Amorphous Calcium Phosphate), prevents conversion to apatite and other less soluble calcium phosphates [28,29]. From a compositional point of view, biological apatites are always carbonated. Natural bone, dentin and enamel contain approximately 7.4, 5.6 and 3.5 wt% of carbonate. Recently, carbonated hydroxyapatite materials have been manufactured *via* various techniques. The most popular are wet chemical methods and solid-state reactions [30,31]. Depending on the technique, powders with different morphologies, stoichiometry and crystallinity can be obtained. Controlling the level of carbonate substitution in hydroxyapatite structure is an effective way to change solubility and morphology of synthesized carbonated HA crystals, which affects properties of HA-based materials [32]. Carbonated hydroxyapatite exhibits higher cell resorption rate *in vitro* which is similar to the resorption rate of natural bone minerals. In synthetic apatites the synergistic effect of Mg and CO_3 on reducing crystallinity and increasing the extent of dissolution has been confirmed [33].

The main goal of our studies was to obtain the new composite type self-setting implant material based on Mg^{2+}/CO_3^{2-} co-substituted hydroxyapatite (MgCHA) and calcium sulfate hemihydrate (CSH). Calcium sulfate hemihydrate is a well-known biodegradable and biocompatible bone defect filler. Much more stable in the living body hydroxyapatite phase, owing to specific structure modification (synergistic effect of magnesium and carbonate ions substitution), seems to be an interesting component of chemically bonded composites for bone grafts. The biomaterial in the form of setting and hardening paste was developed. The influence of initial heat treatment of MgCHA powder and the kind of liquid setting phase on the properties of the new potential biomaterial was determined.

2. Materials and methods

Carbonate hydroxyapatite powder doped with Mg^{2+} ions was produced by the wet chemical method. In the synthesis, CaO, $(NH_4)_2HPO_4$, $(CH_3COO)_2Mg$ and NH_4HCO_3 were applied as sources of calcium, phosphorus, magnesium ions and carbonate groups. The synthesis of MgCHA powder has been described in detail in our previous paper [34]. Briefly, the amounts of the above reagents were 0.51, 0.30, 0.0062 and 0.10 mol, respectively. The Ca/P molar ratio in all precipitates was equal to 1.67. CaO was stirred in 1000 mL of distilled water to produce $Ca(OH)_2$ suspension, while other reagents were dissolved in 1000 mL of distilled water. During synthesis, the pH value of the mixtures was stabilized at $\geq$11 using ammonium hydroxide solution. The suspension was aged for 24 h at room temperature and decanted. The resultant precipitate was washed with distilled water, filtered and dried at 90 °C. The initial MgCHA powder was ground to the size below 0.06 mm. In our studies non-calcined and calcined in air for 2 h at 400 °C modified hydroxyapatite powders were used. The cement powder phase was prepared by mixing MgCHA and CSH powders in the weight ratio of 2:3 under dry conditions in the ball mill (MM 200 Retsch) for 5 min at the frequency of 5 Hz. Non-calcined MgCHA powder was used to prepare cement A, while calcined MgCHA powder – to prepare cement B. Calcium sulfate hemihydrate – CSH (POCH, Poland) was applied as the second component. Distilled water as well as 1.0% chitosan solution in 0.3% acetic acid (Aldrich, Germany) served as liquid phases. The liquid/powder ratio (L/P) was equal to 0.54 mL g^{-1}.

Phase composition was characterized by X-ray diffraction (X'Pert Pro Panalitical diffractometer, Philips). XRD measurements were performed using monochromatic CuK_α radiation within the 2θ range from 10 to 60° at a scanning speed of 10° min^{-1}. Phase quantification and dimensions of crystallographic unit cell were calculated by the Rietveld method. FTIR investigations were conducted on a BIO-RAD FTS-60V spectrometer in the wavenumber range of 4000–400 cm^{-1}. Transmission technique was applied and the samples were prepared as standard KBr pellets. The setting times of the cement pastes were determined using Gilmore Apparatus according to the ASTM C266-08 standard. A light and thick needle of 113.4 g weight and 2.13 mm in diameter was used to measure the initial setting time (I) and the heavy and thin needle of 453.6 g weight and 1.06 mm in diameter for establishing the final setting time (F). Specific surface area of the powder before and after calcination was determined by BET method (ASAP 2010 Micromeritics). Apatite crystals were observed using transmission electron microscopy (TEM; JEOL JEM 1220). A scanning electron microscope (SEM – Nova 200 NanoSEM,

Table 1
ICP-OES instrumental conditions.

Plasma	Argon
Nebulizer gas flow rate	0.8 L min^{-1}
Auxiliary gas flow rate	0.2 L min^{-1}
Plasma gas flow rate	15.0 L min^{-1}
RF Generator power	1300 W
Flow rate of sample	1.5 mL min^{-1}
Plasma observation	Axial (Mg, Ca P I S), radial (Na, K)
Reading parameters	Peak area, 5 points per peak
Measurements	3 replicates, reading time – auto

FEI Company) equipped with X-ray dispersive spectroscopy (EDS) was used to determine crystal morphology and chemical elemental composition in microareas of the cement samples after incubation in SBF (Simulated Body Fluid). The open porosity and pore size distribution were evaluated by Hg porosimeter (Autopore 9500, Micromeritics). For the compressive strength testing, the cement samples (6 mm in diameter and 12 mm high) stored at 37 °C for 1 week were investigated. The compressive strength was measured at a crosshead displacement rate of 2.0 mm min^{-1} using universal materials testing machine Instron 3345. Chemical stability of MgCHA cement was evaluated *in vitro* by measuring pH and ionic conductivity *vs.* time of immersion of the samples in SBF and distilled water using pH/conduct-meter Hanna H198129 Combo. The cylindrical samples (12 mm in diameter and 4 mm high) after 60 min of hardening were placed into the container with 40 mL of SBF or distilled water and stored at 37 °C for 28 days. After the pre-selected soaking time in SBF, the samples were gently rinsed with distilled water to remove SBF solution followed by drying at 40 °C. Sample surfaces were characterized by SEM and EDS for evaluation *in vitro* bioactivity. The concentration of Ca, Mg, K, Na, S, P ions in simulated body fluid solutions (pH 7.4) at 37 °C after 1, 3 and 7 days of hardened bodies incubation was determined. The measurements were performed by a simultaneous inductively coupled plasma optical emission spectrometry (ICP OES) using Perkin Elmer (USA) spectrometer Optima 2100. The ICP conditions are shown in Table 1.

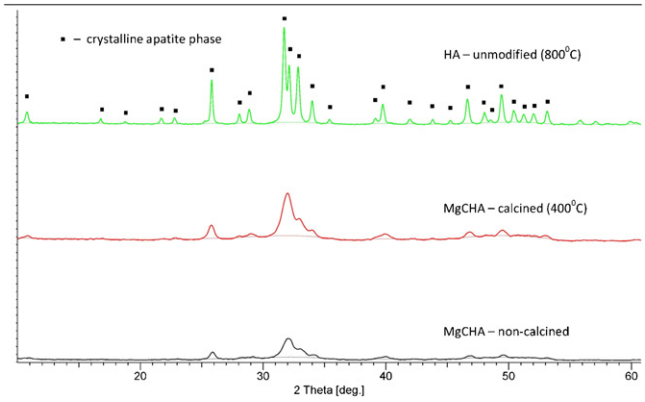

Fig. 1. XRD patterns of HA and MgCHA powders.

3. Results and discussion

The XRD analysis of MgCHA powder revealed no secondary phases (Fig. 1) apart from the apatite phase. Simultaneous incorporation of CO_3^{2-} and Mg^{2+} ions resulted in change of the unit cell parameters *a* and *c* of doped hydroxyapatite as compared to non-modified HA. A decrease in the *a* parameter from 0.94187 to 0.93815 nm and an increase in the *c* parameter from 0.68827 to 0.68929 nm indicate formation of carbonated hydroxyapatite with domination of type B substitution [35]. This finding was confirmed by earlier FTIR study [36]. Non-calcined MgCHA is a nanocrystalline powder (Fig. 2) showing an average grain diameter equal to D_{BET} = 19 nm. Specific surface area measured by conventional BET method for non-calcined and calcined MgCHA powders was equal to 99.8 ± 0.2 and 74.3 $m^2\ g^{-1}$, respectively.

The second powder component, calcium sulfate hemihydrate ($CaSO_4{\cdot}0.5H_2O$), was used as the setting agent. The corresponding setting reaction is as follows:

$$\underset{(CSH)}{CaSO_4{\cdot}0.5H_2O} + 1.5H_2O \rightarrow \underset{(CSD)}{CaSO_4{\cdot}2H_2O} \quad (1)$$

Calcium sulfate hemihydrate reacts with water which leads to calcium sulfate dihydrate formation, partial recrystallization and hardening. Calcium sulfate dihydrate (CSD) is chemically and crystallographically similar to DCPD ($CaHPO_4{\cdot}2H_2O$) and a relatively soluble calcium-rich phase [37]. *In vivo* conditions CSD can form calcium deficient hydroxyapatite (CDHA) (2) or hydroxyapatite (HA) (3) by dissolution and reaction with the phosphate ions present in body fluids [38].

$$9\underset{(CSD)}{CaSO_4 \cdot 2H_2O} + 6HPO_4^{2-} \rightarrow \underset{(CDHA)}{Ca_9(PO_4)_5(HPO_4)OH} + 6H^+ + 9SO_4^{2-} + 17H_2O \quad (2)$$

$$10\underset{(CSD)}{CaSO_4 \cdot 2H_2O} + 6HPO_4^{2-} \rightarrow \underset{(HA)}{Ca_{10}(PO_4)_6(OH)_2} + 8H^+ + 10SO_4^{2-} + 18H_2O \quad (3)$$

These reactions of CSD can be potential factors that initiate bone growth in the places where CSD crystals have been dissolved and replaced by pores.

Table 2 shows initial composition and setting times of the studied new cement-type implant materials. The powders (MgCHA + CSH) and the liquid phases (distilled water or chitosan solution) were mixed together with L/P ratio of 0.54 mL g^{-1}. The cement-type materials set from 7 to 37 min. Initial (I) and final (F) setting times depended on a type of liquid phase and the kind of MgCHA powder applied (calcined or non-calcined). Using distilled water as a liquid phase, heat treatment of the initial magnesium-carbonate hydroxyapatite powder and decreasing its amorphous character resulted in shorter setting times. It was a consequence of higher rate of calcium sulfate hemihydrate hydration process. MgCHA nanopowder reveals high affinity to water which adsorbs on the surface of grains and influences cement setting reaction.

Table 2
Initial phase composition and setting times of the cements.

Cement	Composition of powders	Liquid phase	L/P [mL g^{-1}]	Setting time [min]	
				Initial	Final
A	MgCHA/CSH 2:3	Distilled water	0.54	12	24
		Chitosan solution	0.54	17	37
B	MgCHA-calcined/CSH 2:3	Distilled water	0.54	7	14
		Chitosan solution	0.54	9	18

High specific surface area of non-calcined hydroxyapatite powder is therefore the main reason for its higher reactivity.

The use of chitosan solution as the liquid phase, despite longer setting times of tested samples, had an advantageous impact on the consistency of cement type materials, making them more handy. Chitosan, which is soluble in acidic aqueous media, is used in many biomedical and pharmaceutical applications. The chemical structure and relevant biological properties, such as biocompatibility and non-toxicity as well as antibacterial and antitumor activity makes chitosan a promising candidate for scaffolds for cartilage, intervertebral disc and bone tissue engineering in clinical practice. Moreover, the ability to link chitosan to DNA molecules renders this material a good potential as a substrate for gene activated matrices in gene therapy [39–41].

Phase composition of the hardened cements determined by XRD method revealed the presence of calcium sulfate dihydrate (67 wt% – cement A; 66 wt% – cement B) and hydroxyapatite as the second phase (33 wt% – cement A; 34 wt% – cement B). Infrared spectra of MgCHA-CSD with the distilled water used as a liquid phase are shown in Fig. 3. The spectrum exhibits absorption features at 1452, 1421 and 874 cm^{-1} assigned to the type B apatites (carbonate ions substitution for phosphate ions in the hydroxyapatite structure). Additional band at 1500 cm^{-1} in the infrared spectrum is characteristic for mixed AB type structure. FTIR spectrum shows also the bands originating from PO_4^{3-} ions stretching vibrations at 1042 cm^{-1} (ν_3), 963 cm^{-1} (ν_1) and bending vibrations at 575 cm^{-1} (ν_4). The spectrum of cement exhibits a strong doublet near 604 and 670 cm^{-1} due to the SO_4 bending vibrations (ν_4). The strongest bands are assigned to SO_4 stretching vibrations (ν_3) and can be observed as a doublet near 1121 and 1140 cm^{-1}. Water vibrations are seen at 3548 and 3407 cm^{-1}. There are also two bands characteristic for O–H bending vibrational modes at 1686 and 1623 cm^{-1}. The presence of these two bands indicates existence of two distinct crystallographic types of water – one connected to sulfate ions by hydrogen bonding (the corresponding peak shows lower frequency) and the other one directly linked to calcium ions.

Fractured samples of the hardened cement bodies are presented in Fig. 4. Formation of big, needle-like crystals of gypsum can be observed. Furthermore, micro-areas containing the doped hydroxyapatite in the form of agglomerates can be seen. SEM observations evidenced the influence of the liquid phase and heat-treatment process on the microstructure of the analyzed implant materials. Application of chitosan solution as a liquid phase resulted in faster creation of bioactive apatitic layer on the cement surface, during the samples incubation in SBF at 37 °C. Microscopic observations showed that in the case of cement A, when distilled water was used as a liquid phase, after 2 weeks of immersion in simulated body fluid, well crystallized calcium sulfate dihydrate crystals can still be seen (Fig. 5a). When chitosan solution was used as a liquid phase as early as one week after incubation in SBF, the thick apatitic layer, distributed evenly on the whole cement samples can be observed (Fig. 6). Higher bioactive potential of cement may result from better solubility caused not only by the phase

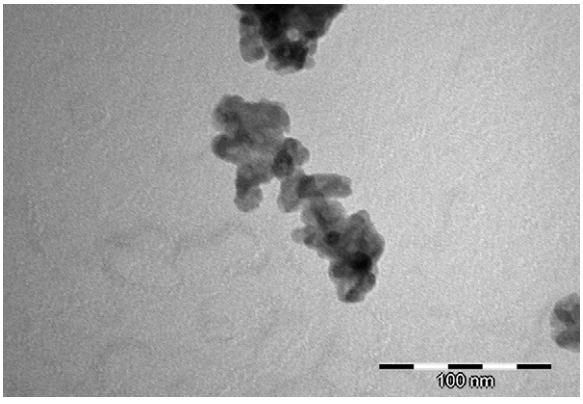

Fig. 2. TEM image of non-calcined MgCHA powder.

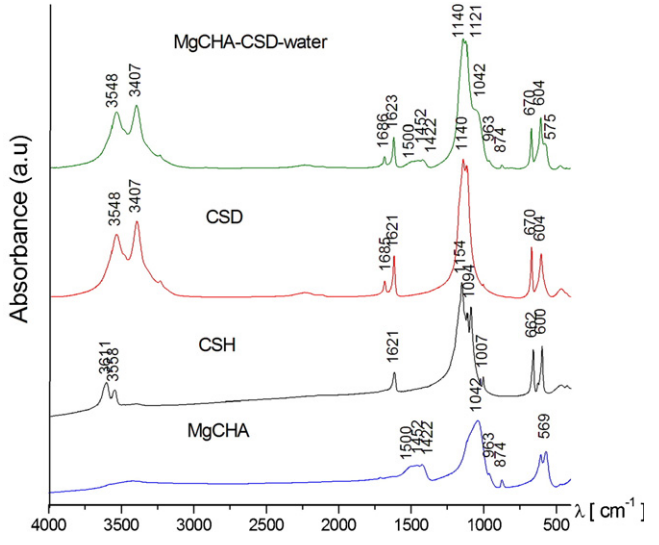

Fig. 3. FTIR spectra of MgCHA, CSH, CSD and MgCHA-CSD with distilled water used as a liquid phase.

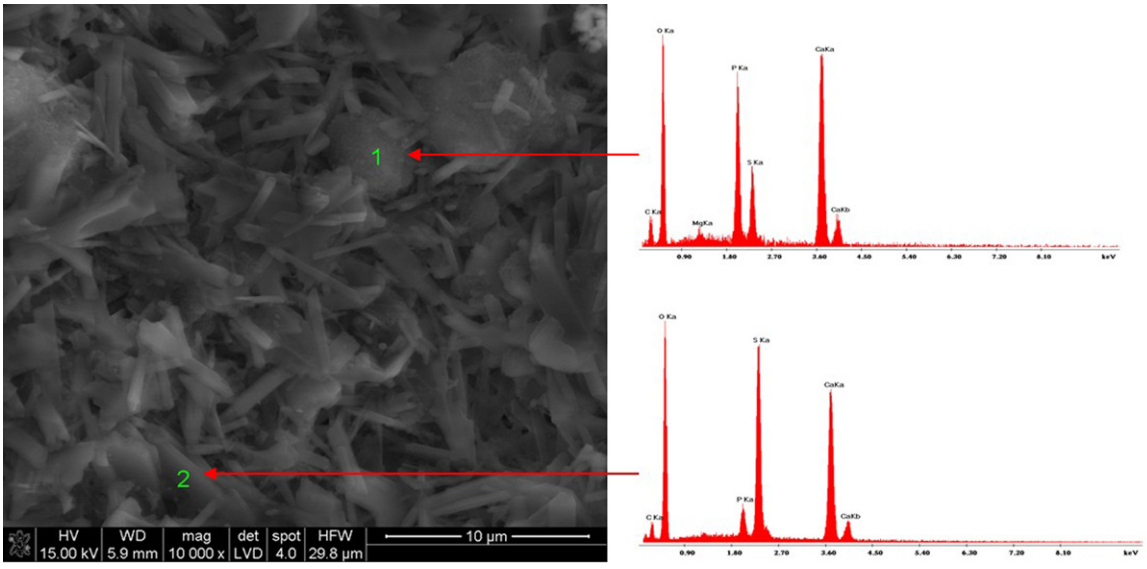

Fig. 4. SEM micrograph and EDS analysis of cement B (chitosan solution was used as a liquid phase).

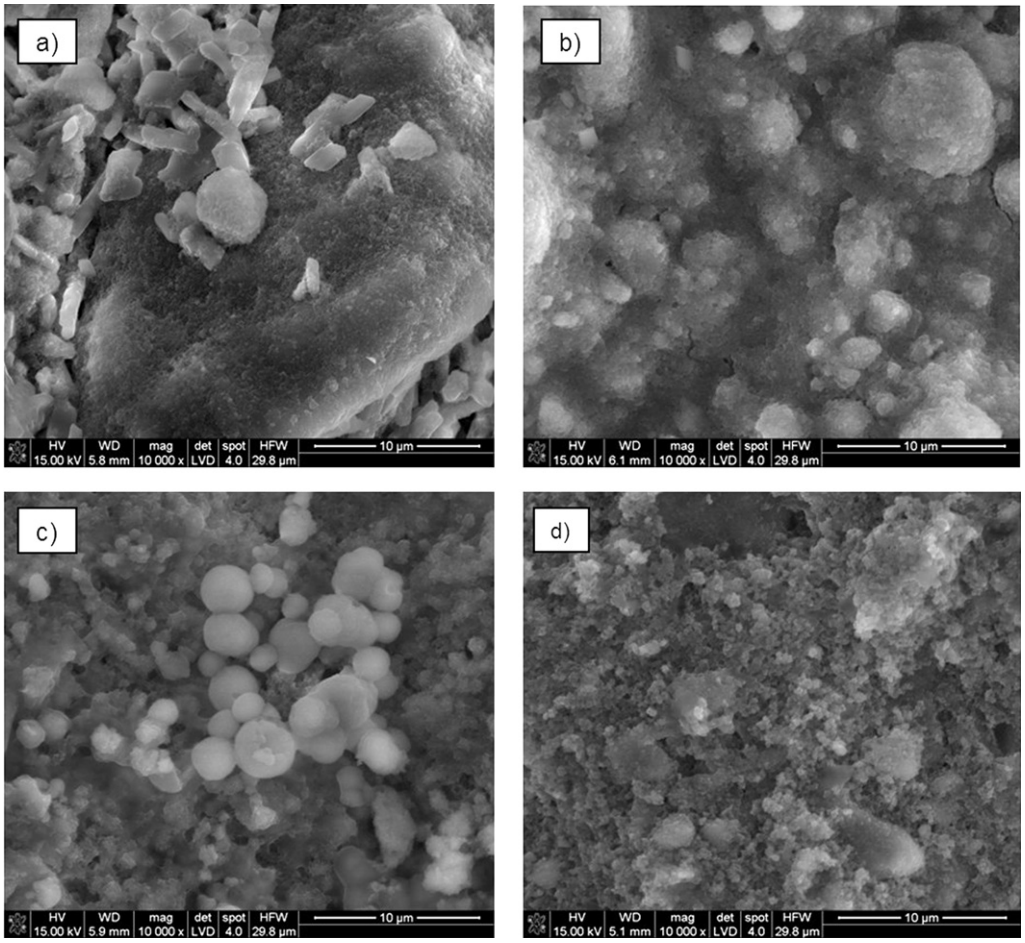

Fig. 5. SEM micrograph of (a) cement A (distilled water was used as a liquid phase) after 2 weeks of incubation in SBF, (b) cement B (distilled water was used as a liquid phase) after 2 weeks of incubation in SBF, (c) cement A (chitosan solution was used as a liquid phase) after 2 weeks of incubation in SBF, and (d) cement B (chitosan solution was used as a liquid phase) after 2 weeks of incubation in SBF.

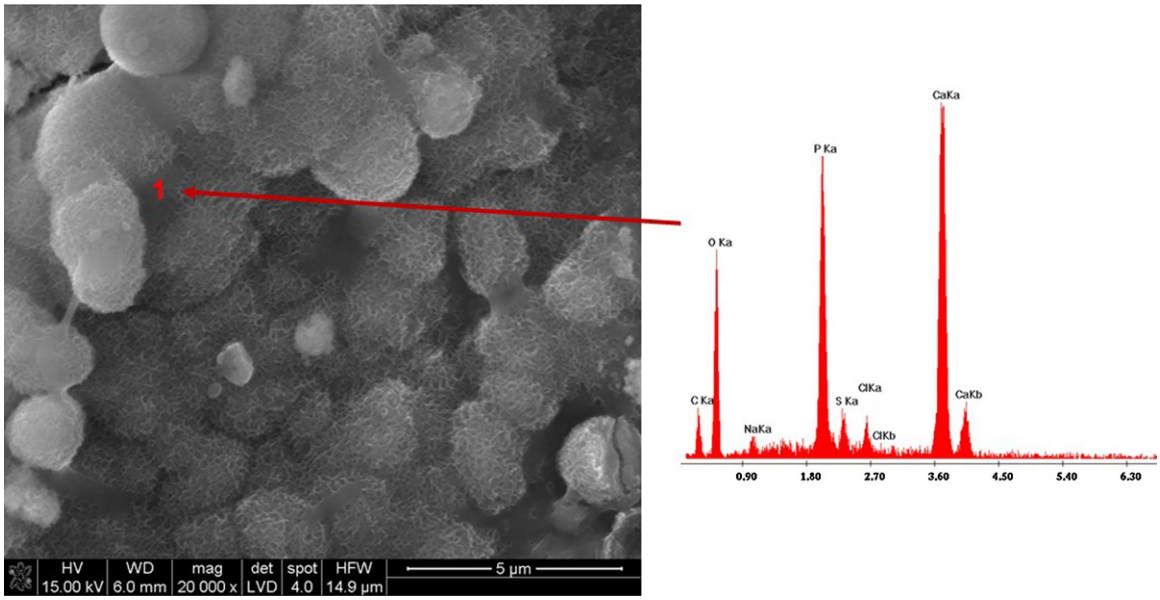

Fig. 6. SEM micrograph and EDS analysis of cement A after a 1 week incubation in SBF (chitosan solution was used as a liquid phase).

Table 3
Properties of bone cements.

Cement	Liquid phase	Phase composition [wt%]		Open porosity [%]	Pore size diameter [µm]
		HA ($Ca_{10}(PO_4)_6(OH)_2$)	CSD ($CaSO_4{\cdot}2H_2O$)		
A	Distilled water	33	67	46	0.008–0.021 0.270–1.100
	Chitosan solution	33	67	44	0.007–0.024 0.250–1.500
B	Distilled water	34	66	46	0.008–0.023 0.250–1.000
	Chitosan solution	34	66	46	0.008–0.024 0.230–0.980

composition (due to dissolution of calcium sulfate dihydrate phase), but also by properties of chitosan used as a liquid phase. After a 4 week incubation in distilled water and SBF the surface of all studied materials was covered with calcium phosphate coatings.

Table 3 summarizes the results of phase composition, open porosity and pore size diameter of the examined cements. There were no significant differences in open porosity between A and B cements. After setting and hardening the studied materials exhibited ~46% open porosity and showed a bimodal pore size distribution (Fig. 7). The highest compressive strength (11.7 ± 0.9 MPa) of the final materials was obtained for the cement based on calcined MgCHA powder and chitosan solution used as a liquid phase (Fig. 8). In most clinical applications, calcium phosphate cements are in direct contact with human trabecular bones. The strength of trabecular bone is close to 10 MPa, so it may be concluded that mechanical requirement for the strength of the cements must be at least as

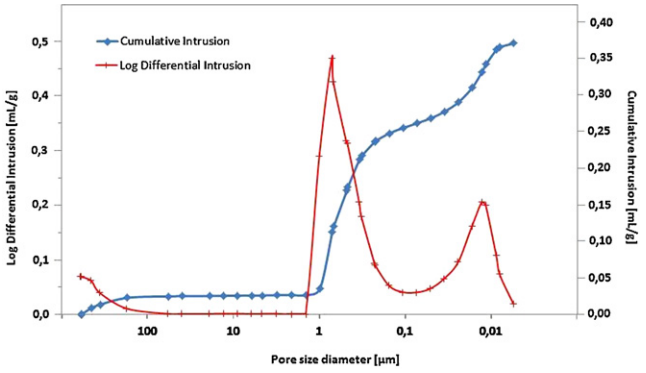

Fig. 7. Pore size distribution of the sample based on MgCHA/CSH and chitosan solution used as liquid phase.

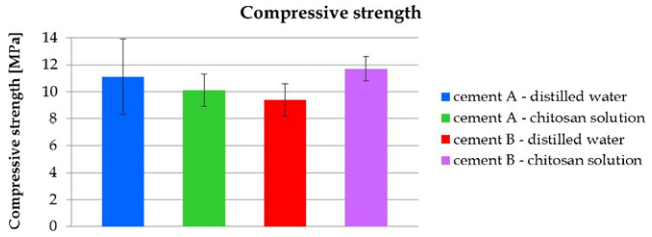

Fig. 8. Compressive strength of the obtained materials 1 week after setting and hardening.

Table 4
Concentrations of various ions in SBF solution after immersion of cement samples.

Material	Day	Ca [mg L^{-1}]	K [mg L^{-1}]	Mg [mg L^{-1}]	Na [mg L^{-1}]	S [mg L^{-1}]	P [mg L^{-1}]
SBF (control)	0	86.18	255.88	38.99	3636.61	12.36	34.97
SBF with MgCHA-calcined/CSH distilled water as liquid phase	1	335.50	242.98	53.27	3571.98	288.33	10.90
	3	518.45	249.72	54.00	3581.58	399.34	2.36
	7	776.86	251.81	57.29	3708.22	565.34	8.21
SBF with MgCHA-calcined/CSH chitosan solution as liquid phase	1	347.78	243.62	54.51	3600.37	260.24	22.44
	3	538.21	249.45	56.95	3704.67	424.67	25.87
	7	699.96	248.16	55.55	3603.46	613.70	10.47

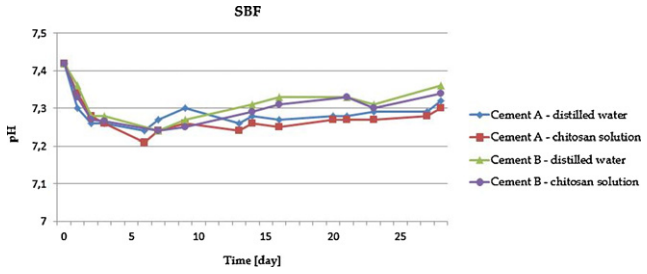

Fig. 9. pH *vs.* time of incubation in SBF.

high as this value. There are also bone cements with lower strength available on the market. For example, commercial cements Cementek and alfa-BSM show the compressive strength of 8 ± 2 MPa and 4 ± 1 MPa, respectively [42].

Chemical stability of the obtained materials was evaluated by pH changes of simulated body fluid (SBF) (Fig. 9) as well as by ionic conductivity changes of distilled water in which the cement samples were incubated (Fig. 10). During 28 days of incubation in SBF no significant pH changes were observed. pH value changed in the range from 7.45 (maximum value) to 7.20 (minimum value) and remained close to the physiological one.

Ionic conductivity of the aqueous extract of the studied materials was high (up to 2250 $\mu S\ cm^{-1}$) and after 15 days it stabilized at the value of 2100 $\mu S\ cm^{-1}$. The increase followed by the decrease in ionic conductivity indicated dissolution and precipitation of apatite from the solution on the surface of the cement samples. The reached level of ionic conductivity resulted from the presence of calcium sulfate as a biodegradable component of cements. This finding was confirmed by ICP-OES analysis. The variation of Ca, S, K, Mg, Na, P ions concentration in SBF solution, before and after 1, 3 and 7 days of immersion of cement samples is shown in Table 4. The increase of Ca (approximately 10 times) and S ions (~50 times) concentrations after 7 days of samples immersion in SBF indicated intensive dissolution of calcium sulfate dihydrate. Lower amount of P ions is probably connected with apatite formation on the cement surface.

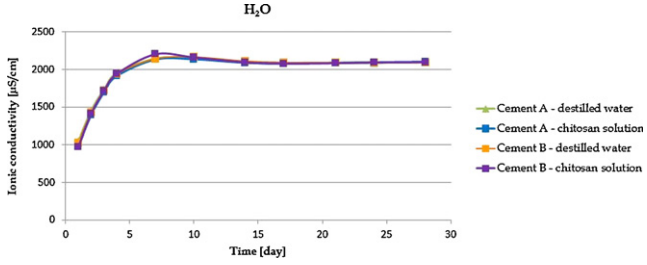

Fig. 10. Ionic conductivity *vs.* time of incubation in distilled water.

4. Conclusions

In this study the new cement-type composite implant material based on Mg^{2+}/CO_3^{2-} co-substituted hydroxyapatite (MgCHA) and calcium sulfate hemihydrate (CSH) was developed. The results concerning the studied material can be summarized as follows:

- The investigated bone cement reveals good surgical handiness and can be applied to repair bone defects.
- Initial (I) and final (F) setting times of the cement depend on the type of the liquid phase (distilled water or chitosan solution) and the kind of MgCHA powder applied (calcined or non-calcined).
- Heat treatment of the initial magnesium-carbonate hydroxyapatite powder results in shorter setting times of the MgCHA-CSH pastes.
- After setting and hardening, porous material (porosity ~46%) with bimodal pore size distribution in the range of 0.007–1.5 μm is obtained.
- The studied composite is bioactive and chemically stable (during 28 days of incubation in SBF, pH of the solutions remained close to the physiological value 7.4).
- The produced bone substitute is an alternative to autografts. Due to the presence of biodegradable calcium sulfate and more soluble amorphous MgCHA the new material seems to reveal tendency to faster resorption with respect to previous CPC materials. This requires confirmation in biological tests.

Acknowledgments

The authors would like to thank to Dr. Cz. Paluszkiewicz for the FTIR measurements and Prof. M.M. Bućko for XRD studies.

This work has been supported by the project No. UDA-POIG.01.03.01-00-005/09.

References

[1] M.P. Ginebra, M. Espanol, E.B. Monfutar, R.A. Perez, G. Mestres, New processing approaches in calcium phosphate cements and their applications in regenerative medicine, Acta Biomaterialia 6 (2010) 2863–2873.

[2] M. Bohner, U. Gbureck, J.E. Barralet, Technological issues for the development of more efficient calcium phosphate bone cements: a critical assessment, Biomaterials 26 (2005) 6423–6429.
[3] A. Tofighi, K. Schaffer, R. Pallazzolo, Calcium phosphate cement (CPC): a critical development path, Key Engineering Materials 361–363 (2008) 303–306.
[4] S. Dorozhkin, Bioceramics of calcium orthophosphates, Biomaterials 31 (2010) 1465–1485.
[5] A. Ambard, L. Mueninghoff, Calcium phosphate cement: review of mechanical and biological properties, Journal of Prosthodontics 15 (2006) 321–328.
[6] T. Chiang, C. Ho, D. Chan-Hen Chen, M. Lai, S. Ding, Physicochemical properties and biocompatibility of chitosan oligosaccharide/gelatin/calcium phosphate hybrid cements, Materials Chemistry and Physics 120 (2010) 282–288.
[7] M. Bohner, Calcium orthophosphate in medicine: from ceramic to calcium phosphate cements, Injury – International Journal of the Care of the Injured 31 (2000) 37–47.
[8] J.T. Zhang, F. Tancret, J.M. Bouler, Fabrication and mechanical properties of calcium phosphate cements (CPC) for bone substitution, Materials Science and Engineering C 31 (2011) 740–747.
[9] S.V. Dorozhkin, Calcium orthophosphate cement for biomedical application, Journal of Materials Science 43 (2008) 3028–3057.
[10] B. Bourgeois, O. Laboux, L. Obadia, O. Gauthier, E. Betti, E. Aguado, G. Daculsi, J.M. Bouler, Calcium-deficient apatite: a first *in vivo* study concerning bone ingrowth, Journal of Biomedical Materials Research – Applied Biomaterials 65A (2003) 402–408.
[11] S. Wenisch, J.P. Stahl, U. Horas, C. Heiss, O. Kilian, K. Trinkaus, A. Hild, R. Schnettler, *In vivo* mechanisms of hydroxyapatite ceramic degradation by osteoclasts: fine structural microscopy, Journal of Biomedical Materials Research – Applied Biomaterials 63A (2003) 713–717.
[12] L.M. Grover, J.C. Knowles, G.J.P. Fleming, J.E. Barralet, *In vitro* ageing of brushite calcium phosphate cement, Biomaterials 24 (2003) 4133–4141.
[13] D. Apelt, F. Theiss, A. El-Warrak, K. Zlinszky, R. Bettschart-Wolfisberger, M. Bohner, S. Matter, *In vivo* behavior of three different injectable hydraulic calcium phosphate cements, Biomaterials 25 (2004) 1439–1451.
[14] X. Zhidao, L. Grover, *In vitro* biodegradation of three brushite calcium phosphate cements by a macrophage cell-line, Biomaterials 27 (2006) 4557–4565.
[15] F. Theiss, D. Apelt, B. Brand, A. Kutter, M. Zlinszky, M. Bohner, C. Frei, Biocompatibility and resorption of a brushite calcium phosphate cement, Biomaterials 26 (2005) 4383–4394.
[16] P. Frayssinet, L. Gineste, P. Conte, J. Fages, N. Rouquet, Short-term implantation effects of a DCPD-based calcium phosphate cement, Biomaterials 19 (1998) 971–977.
[17] B. Constantz, B. Barr, J. Ison, M. Fulmer, J. Baker, L. McKinney, S. Goodman, S. Gunasekaren, D. Delaney, J. Ross, J. Poser, Histological, chemical, and crystallographic analysis of four calcium phosphate cements in different rabbits osseous sites, Journal of Biomedical Materials Research 43 (1998) 451–461.
[18] B. Flauture, C. Delecourt, M. Blary, P. Van Landuyt, J. Lemaitre, P. Hardoui, Volume effect on biological properties of a calcium phosphate hydraulic cement: experimental study in sheep, Bone 25 (1999) 35–39.
[19] D. Pioletti, H. Takei, T. Lin, P. Van Landuyt, Q. Ma, S. Kwon, K. Sung, The effect of calcium phosphate cement particles on osteoblast function, Biomaterials 21 (2000) 1103–1114.
[20] M. Markovic, S. Takagi, L.C. Chow, Formation of macropores in calcium phosphate cements trought the use of mannitol crystals, Key Engineering Materials 192–195 (2001) 773–776.
[21] J.E. Barralet, L. Grover, T. Gaunt, A.J. Wright, I.R. Gibson, Preparation of macroporous calcium phosphate cement tissue engineering scaffold, Biomaterials 23 (2002) 3063–3072.
[22] H. Xu, J.B. Quinn, Calcium phosphate cement containing restorable fibres for short-term reinforcement and macroporosity, Biomaterials 23 (2002) 193–202.
[23] Y. Zuo, F. Yang, J.G.C. Wolke, Y. Li, J.A. Jansen, Incorporation of biodegradable electrospun fibres into calcium phosphate cement for bone regeneration, Acta Biomaterialia 6 (2010) 1238–1247.
[24] W. Suchanek, M. Yashima, M. Kakihana, M. Yoshimura, Hydroxyapatite ceramics with selected sintering additives, Biomaterials 18 (1997) 923–933.
[25] T.J Webster, E. Massa-Schlueter, J. Smith, E. Slamovich, Osteoblast response to hydroxyapatite doped with divalent and trivalent cations, Biomaterials 25 (2004) 2111–2121.
[26] S. Pina, S. Olhero, S. Gheduzzi, A. Miles, J. Ferreira, Influence of setting liquid composition and liquid-to-powder ratio on properties of a Mg-substituted calcium phosphate cement, Acta Biomaterialia 5 (2009) 1233–1240.
[27] K. Lilley, U. Gbureck, D. Farrar, C. Ansell, J. Barralet, Cement from magnesium substituted hydroxyapatite, Journal of Materials Science-Materials in Medicine 16 (2005) 455–460.
[28] M. Julien, I. Khairoun, R. LeGeros, et al., Physico-chemical-mechanical and *in vitro* biological properties of calcium phosphate cements with doped amorphous calcium phosphate, Biomaterials 28 (2007) 956–965.
[29] R. LeGeros, Calcium phosphates in oral biology and medicine, Monographs in Oral Science, vol.15, Karger, Basel, 1991.
[30] E. Landi, A. Tampieri, M. Mattioli-Belmonte, et al., Biomimetic Mg- and Mg,CO_3-substituted hydroxyapatites: synthesis characterization and *in vitro* behavior, Journal of the European Ceramic Society 26 (2006) 2593–2601.
[31] J. Lafon, E. Champion, D. Bernache-Assollant, Processing of AB-type carbonated hydroxyapatite Ca_{10}-$x(PO_4)_6$-$x(CO_3)_x(OH)_2$-x-$2y(CO_3)y$ ceramics with controlled composition, Journal of the European Ceramic Society 28 (2008) 139–147.
[32] W. Suchanek, P. Shuk, K. Byrappa, R. Riman, K. TenHuisen, V. Janas, Mechanochemical-hydrothermal synthesis of carbonated apatite powders at room temperature, Biomaterials 23 (2002) 699–710.
[33] R.Z. LeGeros, R. Kijkowska, C. Bautista, J. LeGeros., Synergistic effects of magnesium and carbonate on properties of biological and synthetic apatites, Connective Tissue Research 31 (1995) 1–7.
[34] A. Ślosarczyk, Z. Paszkiewicz, C. Paluszkiewicz, FTIR and XRD evaluation of carbonated hydroxyapatite powders synthesized by wet methods, Journal of Molecular Structure 744–747 (2005) 657–661.
[35] R.Z. LeGeros, in: P.W. Brown, B. Constanz (Eds.), Hydroxyapatite and Related Materials, CRC Press, Boca Raton, 1994, pp. 3–28.
[36] J. Kolmas, A. Jaklewicz, A. Zima, M. Bućko, Z. Paszkiewicz, J. Lis, A. Ślósarczyk, W. Kolodziejski, Incorporation of carbonate and magnesium ions into synthetic hydroxyapatite: the effect on physicochemical properties, Journal of Molecular Structure 987 (2011) 40–50.
[37] W. Heijnen, P. Hartman, Structural morphology of gypsum ($CaSO_4 \cdot 2H_2O$), brushite ($CaHPO_4 \cdot 2H_2O$) and pharmacolite (CaHA-$sO_4 \cdot 2H_2O$), Journal of Crystal Growth 108 (1991) 290–300.
[38] M. Bohner, New hydraulic cements based on α-tricalcium phosphate-calcium sulfate dihydrate mixtures, Biomaterials 25 (2004) 741–749.
[39] M. Rinaudo, Chitin and chitosan: properties and applications, Progress in Polymer Science 31 (2006) 603–632.
[40] A. Di Martino, M. Sittinger, M. Risbud, Chitosan: a versatile biopolymer for orthopaedic tissue-engineering, Biomaterials 26 (2005) 5983–5990.
[41] M. Dash, F. Chiellini, R. Ottenbrite, E. Chiellini, Chitosan: a versatile semi-synthetic polymer in biomedical applications, Progress in Polymer Science 36 (2011) 981–1014.
[42] S. Dorozhkin, Calcium orthophosphate cements for biomedical application, Journal of Materials Science 43 (2008) 3028–3057.